



1        **Stable isotopic evidence for the excess leaching of unprocessed atmospheric**  
2        **nitrate from forested catchments under high nitrogen saturation**

Weitian Ding<sup>1</sup>, Urumu Tsunogai<sup>1</sup>, Fumiko Nakagawa<sup>1</sup>, Takashi Sambuichi<sup>1</sup>, Masaaki  
Chiwa<sup>2</sup>, Tamao Kasahara<sup>3</sup>, Ken'ichi Shinozuka<sup>4</sup>

<sup>1</sup>Graduate School of Environmental Studies, Nagoya University, Furo-cho, Chikusa-ku,  
Nagoya 464-8601, Japan

<sup>2</sup>Kyushu University Forest, Kyushu University

<sup>3</sup>Faculty of Agriculture, Kyushu University

<sup>4</sup>River Basin Research Center, Gifu University, 1-1 Yanagido, Gifu, 501-1193, Japan

Corresponding author: Weitian Ding

Email: [ding.weitian.v2@s.mail.nagoya-u.ac.jp](mailto:ding.weitian.v2@s.mail.nagoya-u.ac.jp)



### 3 Abstract

4 The average concentration of stream nitrate eluted from the FK forested catchments  
5 (FK1 and FK2) in Japan was more than 90  $\mu\text{M}$ , implying that these forested catchments  
6 were under nitrogen saturation. To verify that these forested catchments were under the  
7 nitrogen saturation, we determined the export flux of unprocessed atmospheric nitrate  
8 relative to the entire deposition flux ( $M_{\text{atm}}/D_{\text{atm}}$  ratio) in these catchments, because the  
9  $M_{\text{atm}}/D_{\text{atm}}$  ratio has recently been proposed as a reliable index to evaluate nitrogen  
10 saturation in forested catchments. Specifically, we determined the temporal variation in  
11 the concentrations and stable isotopic compositions, including  $\Delta^{17}\text{O}$ , of stream nitrate  
12 in the FK catchments for more than 2 years. In addition, for comparison, the same  
13 parameters were also monitored in the MY forested catchment in Japan during the same  
14 period, where the average stream nitrate concentration was low, less than 10  $\mu\text{M}$ . While  
15 showing the average nitrate concentrations of 109.5, 94.2, and 7.1  $\mu\text{M}$  in FK1, FK2,  
16 and MY, respectively, the catchments showed average  $\Delta^{17}\text{O}$  values of +2.6, +1.7, and  
17 +0.6 ‰ in FK1, FK2, and MY, respectively. Thus, the average concentration of  
18 unprocessed atmospheric nitrate ( $[\text{NO}_3^-]_{\text{atm}}$ ) was estimated to be 10.8, 6.1, and 0.2  $\mu\text{M}$   
19 in FK1, FK2, and MY, respectively, and the  $M_{\text{atm}}/D_{\text{atm}}$  ratio was estimated to be 13.9,  
20 7.9, and 1.2 % in FK1, FK2, and MY, respectively. The estimated  $M_{\text{atm}}/D_{\text{atm}}$  ratio in  
21 FK1 (13.9 %) was the highest ever reported from temperate forested catchments  
22 monitored for more than 1 year. Thus, we concluded that nitrogen saturation was  
23 responsible for the enrichment of stream nitrate in the FK catchments, together with the



24 elevated  $\text{NO}_3^-$  atm leaching from the catchments. While the stream nitrate concentration  
25 ( $[\text{NO}_3^-]$ ) can be affected by the amount of precipitation, the  $M_{\text{atm}}/D_{\text{atm}}$  ratio is  
26 independent of the amount of precipitation; thus, the  $M_{\text{atm}}/D_{\text{atm}}$  ratio can be used as a  
27 robust index for evaluating nitrogen saturation in forested catchments.

28

## 29 **1 Introduction**

30 Nitrate is important as a nitrogenous nutrient in the biosphere. Traditionally, forested  
31 ecosystems have been considered as nitrogen limited (Vitousek and Howarth, 1991).  
32 However, owing to the elevated loading of nitrogen through atmospheric deposition,  
33 some forested ecosystems become nitrogen saturated (Aber et al., 1989), from which  
34 elevated levels of nitrate are exported (Mitchell et al., 1997; Peterjohn et al., 1996).  
35 Such excessive leaching of nitrate from forested catchments degrades water quality and  
36 causes eutrophication in downstream areas (Galloway et al., 2003; Paerl and Huisman,  
37 2009). Thus, evaluating the stage of nitrogen saturation in each forested catchment  
38 including its temporal variation, is critical for sustainable forest management,  
39 especially for forested ecosystems under high nitrogen deposition.

40 Both concentration and seasonal variation of stream nitrate have been used as indexes  
41 to evaluate the nitrogen saturation of each forested catchment in past studies (Aber,  
42 1992; Rose et al., 2015; Stoddard, 1994). A forested stream eluted from Fernow  
43 Experimental Forest USA, for instance, showed an elevated average nitrate  
44 concentration of  $60 \mu\text{M}$ , along with the absence of a seasonal variation in the stream



45 nitrate concentration, so the forest was classified into stage 3, the highest stage of  
46 nitrogen saturation (Rose et al., 2015).

47 However, using both the concentration level (high or low) and seasonal variation  
48 (clear or absent) of stream nitrate as indexes to evaluate nitrogen saturation has  
49 limitations, including the following (1) seasonal variation of stream nitrate can be  
50 buffered by groundwater in forests under humid, temperate climates such as Japan, so  
51 the seasonal variation in stream nitrate concentrations is unclear, even in normal forests  
52 under the nitrogen saturation stage of 0 (Mitchell et al., 1997); and (2) the stream nitrate  
53 concentration can be enriched or diluted depending on the volume of rainfall, so the  
54 concentration level can be high in low precipitation area irrespective of the stage of  
55 nitrogen saturation.

56 Nakagawa et al. (2018) lately proposed that the  $M_{\text{atm}}/D_{\text{atm}}$  ratio, the export flux of  
57 unprocessed atmospheric nitrate ( $M_{\text{atm}}$ ) relative to the deposition flux of  $\text{NO}_3^-_{\text{atm}}$  ( $D_{\text{atm}}$ ),  
58 can be an alternative, more robust index for evaluating nitrogen saturation in each  
59 forested catchment, because the  $M_{\text{atm}}/D_{\text{atm}}$  ratio directly reflects the demand for  
60 atmospheric nitrate deposited onto each forested catchments as a whole, and thus reflect  
61 the nitrogen saturation in each forested catchment. That is, we can expect high  
62  $M_{\text{atm}}/D_{\text{atm}}$  ratios in forested catchments under nitrogen saturation and low  $M_{\text{atm}}/D_{\text{atm}}$   
63 ratios in forested catchments with nitrogen deficiency.

64 To estimate the  $M_{\text{atm}}/D_{\text{atm}}$  ratio accurately and precisely in each forested catchment,  
65 the fraction of unprocessed atmospheric nitrate ( $\text{NO}_3^-_{\text{atm}}$ ) in the stream needs to be



66 estimated accurately and precisely. In recent, triple oxygen isotopic compositions of  
67 nitrate ( $\Delta^{17}\text{O}$ ) have been used as a conservative tracer of  $\text{NO}_3^-_{\text{atm}}$  deposited onto each  
68 forested catchment (Inoue et al., 2021; Michalski et al., 2004; Nakagawa et al., 2018;  
69 Tsunogai et al., 2014; Ding et al., 2022), showing distinctively different  $\Delta^{17}\text{O}$  from that  
70 of remineralized nitrate ( $\text{NO}_3^-_{\text{re}}$ ), derived from organic nitrogen through general  
71 chemical reactions, including microbial N mineralization and microbial nitrification.  
72 While  $\text{NO}_3^-_{\text{re}}$ , the oxygen atoms of which are derived from either terrestrial  $\text{O}_2$  or  $\text{H}_2\text{O}$   
73 through microbial processing (i.e., nitrification), always shows the relation close to the  
74 “mass-dependent” relative relation between  $^{17}\text{O}/^{16}\text{O}$  ratios and  $^{18}\text{O}/^{16}\text{O}$  ratios;  $\text{NO}_3^-_{\text{atm}}$   
75 displays an anomalous enrichment in  $^{17}\text{O}$  reflecting oxygen atom transfers from  
76 atmospheric ozone ( $\text{O}_3$ ) during the conversion of  $\text{NO}_x$  to  $\text{NO}_3^-_{\text{atm}}$  (Alexander et al.,  
77 2009; Michalski et al., 2003; Morin et al., 2011; Nelson et al., 2018). As a result, the  
78  $\Delta^{17}\text{O}$  signature defined by the following equation (Kaiser et al., 2007) enables us to  
79 distinguish  $\text{NO}_3^-_{\text{atm}}$  ( $\Delta^{17}\text{O} > 0$ ) from  $\text{NO}_3^-_{\text{re}}$  ( $\Delta^{17}\text{O} = 0$ ):

$$80 \quad \Delta^{17}\text{O} = \frac{1 + \delta^{17}\text{O}}{(1 + \delta^{18}\text{O})^\beta} - 1 \quad (1)$$

81 where the constant  $\beta$  is 0.5279 (Kaiser et al., 2007),  $\delta^{18}\text{O} = R_{\text{sample}}/R_{\text{standard}} - 1$  and  $R$  is  
82 the  $^{18}\text{O}/^{16}\text{O}$  ratio (or the  $^{17}\text{O}/^{16}\text{O}$  ratio in the case of  $\delta^{17}\text{O}$  or the  $^{15}\text{N}/^{14}\text{N}$  ratio in the case  
83 of  $\delta^{15}\text{N}$ ) of the sample and each standard reference material. In addition,  $\Delta^{17}\text{O}$  is almost  
84 stable during “mass-dependent” isotope fractionation processes within terrestrial  
85 ecosystems. Therefore, while the  $\delta^{15}\text{N}$  or  $\delta^{18}\text{O}$  signature of  $\text{NO}_3^-_{\text{atm}}$  can be overprinted  
86 by the biological processes subsequent to deposition,  $\Delta^{17}\text{O}$  can be used as a robust tracer



87 of unprocessed  $\text{NO}_3^-_{\text{atm}}$  to reflect its accurate mole fraction within total  $\text{NO}_3^-$ ,  
88 regardless of the progress of the partial metabolism (partial removal of nitrate through  
89 denitrification and assimilation) subsequent to deposition (Michalski et al., 2004;  
90 Nakagawa et al., 2013, 2018; Tsunogai et al., 2011, 2014, 2018).

91 Past studies reported that the maximum concentration of stream nitrate was  $58.4 \mu\text{M}$   
92 in the KJ forested catchment in Japan, with the maximum value of the  $M_{\text{atm}}/D_{\text{atm}}$  ratio  
93 was 9.4 % (Nakagawa et al., 2018; Sase et al., 2022). Whether the index of the  $M_{\text{atm}}/D_{\text{atm}}$   
94 ratio can be applied to forested catchments, where the leaching of stream nitrate is much  
95 higher than the KJ forested catchment, remained unclarified.

96 In recent, Chiwa (2021) has reported the enrichment of nitrate of more than  $90 \mu\text{M}$   
97 on the annual average in forested streams eluted from the FK catchments (FK1 and FK2)  
98 in Kasuya Research Forest, Kyushu University, Japan (Figs. 1a and 1b). The observed  
99 enrichment of stream nitrate implied that these forested catchments were under nitrogen  
100 saturation. Thus, in this study, we determined the  $M_{\text{atm}}/D_{\text{atm}}$  ratio in the FK1 and FK2  
101 forested catchments by monitoring both the concentration and  $\Delta^{17}\text{O}$  of stream nitrate  
102 for more than 2 years to verify that these forested catchments were under nitrogen  
103 saturation. For comparison, the MY forested catchment in Shiiba Research Forest,  
104 Kyushu University, Japan (Figs. 1a and 1c), was also monitored during the same period,  
105 where the average stream nitrate concentration was low (less than  $10 \mu\text{M}$ ). Furthermore,  
106 the  $M_{\text{atm}}/D_{\text{atm}}$  ratios in these forested catchments were compared with those reported in  
107 past studies to verify the reliability of the  $M_{\text{atm}}/D_{\text{atm}}$  ratio as an index of nitrogen



108 saturation.

109

## 110 **2 Methods**

### 111 2.1 Study sites

112 The FK forested catchments (33°38'N, 130°31'E) are located in a suburban area,  
113 about 15 km west of the Fukuoka metropolitan area (the fourth largest metropolitan  
114 area in Japan). The main plantation in these catchments was Japanese cedar/cypress  
115 (Table 1). The MY forested catchment (32°22'N, 131°09'E) is located in a rural area at  
116 the village of Shiiba in southern Japan's Central Kyushu Mountain range. This  
117 catchment is a mixed forest consisting of coniferous trees such as *Abies firma* Sieb. et  
118 *Zucc.*, and *Tsuga sieboldii* Carr., and deciduous broadleaved trees such as *Quercus*  
119 *crispula* Blume, *Fagus crenata* Blume, and *Acer sieboldianum* Miq. The annual average  
120 precipitation was 1769 mm and 3837 mm at FK and MY forested catchment,  
121 respectively, and the annual average temperature was 15.9 °C and 10.8 °C at FK and  
122 MY forested catchment, respectively. Details on the studied forested catchments have  
123 been described in the past studies (Chiwa, 2020, 2021).

124

### 125 2.2 Sampling

126 The stream water eluted from the FK1 (14 ha), FK2 (62 ha), and MY (43 ha)  
127 forested catchments were collected about once every month in principle from 2019/11  
128 to 2021/12 (Fig. 1). At the FK catchments, stream water was collected at upstream (FK1)



129 and downstream (FK2) locations (Fig. 1b). Samples of stream water to determine the  
130 concentration and stable isotopic compositions ( $\delta^{15}\text{N}$ ,  $\delta^{18}\text{O}$ , and  $\Delta^{17}\text{O}$ ) of stream nitrate  
131 were collected manually in bottles washed with deionized water before sampling and  
132 then rinsed at least twice with the sample before sampling at each sampling site.

133

### 134 2.3 Analysis

135 All the stream water samples were passed through a membrane filter (pore size 0.45  
136  $\mu\text{m}$ ) within two days after sampling and stored in a refrigerator (4 °C) until analysis.

137 The concentrations of nitrate were measured by ion chromatography (Prominence  
138 HIC-SP, Shimadzu, Japan). To determine the stable isotopic compositions of nitrate in  
139 the stream water samples, nitrate in each sample was chemically converted to  $\text{N}_2\text{O}$  using  
140 a method originally developed to determine the  $^{15}\text{N}/^{14}\text{N}$  and  $^{18}\text{O}/^{16}\text{O}$  ratios of seawater  
141 and freshwater nitrate (McIlvin and Altabet, 2005) that was later modified (Konno et  
142 al., 2010; Tsunogai et al., 2011; Yamazaki et al., 2011). In brief, 11 mL of each sample  
143 solution was pipetted into a vial with a septum cap. Then, 0.5 g of spongy cadmium  
144 was added, followed by 150  $\mu\text{L}$  of a 1 M  $\text{NaHCO}_3$  solution. The sample was then shaken  
145 for 18-24 h at a rate of 2 cycles  $\text{s}^{-1}$ . Then, the sample solution (10 mL) was decanted  
146 into a different vial with a septum cap. After purging the solution using high-purity  
147 helium, 0.4 mL of an azide-acetic acid buffer, which had also been purged using high-  
148 purity helium, was added. After 45 min, the solution was alkalized by adding 0.2 mL  
149 of 6 M NaOH.





150 Then, the stable isotopic compositions ( $\delta^{15}\text{N}$ ,  $\delta^{18}\text{O}$ , and  $\Delta^{17}\text{O}$ ) of the  $\text{N}_2\text{O}$  in each vial  
151 were determined using the continuous-flow isotope ratio mass spectrometry (CF-IRMS)  
152 system at Nagoya University. The analytical procedures performed using the CF-IRMS  
153 system were the same as those detailed in previous studies (Hirota et al., 2010; Komatsu  
154 et al., 2008a). The obtained values of  $\delta^{15}\text{N}$ ,  $\delta^{18}\text{O}$ , and  $\Delta^{17}\text{O}$  for the  $\text{N}_2\text{O}$  derived from  
155 the nitrate in each sample were compared with those derived from our local laboratory  
156 nitrate standards to calibrate the values of the sample nitrate to an international scale  
157 and to correct for both isotope fractionation during the chemical conversion to  $\text{N}_2\text{O}$  and  
158 the progress of oxygen isotope exchange between the nitrate derived reaction  
159 intermediate and water (ca. 20 %). The local laboratory nitrate standards used for the  
160 calibration had been calibrated using the internationally distributed isotope reference  
161 materials (USGS-34 and USGS-35). In this study, we adopted the internal standard  
162 method to calibrate the stable isotopic compositions of sample nitrate (Ding et al., 2022;  
163 Nakagawa et al., 2013, 2018; Tsunogai et al., 2014).

164 The  $\delta^2\text{H}$  and  $\delta^{18}\text{O}$  values of  $\text{H}_2\text{O}$  of the stream water samples were analyzed using  
165 the cavity ring-down spectroscopy method by employing an L2120-i instrument  
166 (Picarro Inc., Santa Clara, CA, USA) equipped with an A0211 vaporizer and  
167 autosampler. The errors (standard errors of the mean) in this method were  $\pm 0.5\text{‰}$  for  
168  $\delta^2\text{H}$  and  $\pm 0.1\text{‰}$  for  $\delta^{18}\text{O}$ . Both the VSMOW and standard light Antarctic precipitation  
169 (SLAP) were used to calibrate the values to the international scale. The  $\delta^{18}\text{O}$  values of  
170  $\text{H}_2\text{O}$  were used to calibrate the differences in  $\delta^{18}\text{O}$  of  $\text{H}_2\text{O}$  between the samples and



171 those our local laboratory nitrate standard samples (Tsunogai et al., 2010, 2011, 2014).

172 To determine whether the conversion rate from nitrate to N<sub>2</sub>O was sufficient, the  
173 concentration of nitrate in the samples was determined each time we analyzed the  
174 isotopic composition using CF-IRMS based on the N<sub>2</sub>O<sup>+</sup> or O<sub>2</sub><sup>+</sup> outputs. We adopted  
175 the δ<sup>15</sup>N, δ<sup>18</sup>O, and Δ<sup>17</sup>O values only when the concentration measured via CF-IRMS  
176 correlated with the concentration measured via ion chromatography prior to isotope  
177 analysis within a difference of 10 %. We repeated the analysis of δ<sup>15</sup>N, δ<sup>18</sup>O, and Δ<sup>17</sup>O  
178 values for each sample at least three times to attain high precision. All samples had a  
179 nitrate concentration of greater than 3.5 μM, which corresponded to a nitrate quantity  
180 greater than 35 nmol in a 10 mL sample. Thus, all isotope values presented in this study  
181 have an error (standard error of the mean) better than ±0.2 ‰ for δ<sup>15</sup>N, ±0.3 ‰ for δ<sup>18</sup>O,  
182 and ±0.1 ‰ for Δ<sup>17</sup>O.

183 Nitrite (NO<sub>2</sub><sup>-</sup>) in the samples interferes with the final N<sub>2</sub>O produced from nitrate  
184 because the chemical method also converts NO<sub>2</sub><sup>-</sup> to N<sub>2</sub>O (McIlvin and Altabet, 2005).  
185 Therefore, it is sometimes necessary to remove NO<sub>2</sub><sup>-</sup> prior to converting nitrate to N<sub>2</sub>O.  
186 In this study, however, we skipped the processes for removing NO<sub>2</sub><sup>-</sup> because all the  
187 stream samples analyzed for stable isotopic composition had NO<sub>2</sub><sup>-</sup> concentrations lower  
188 than the detection limit (0.05 μM).

189

#### 190 2.4 Deposition rate of atmospheric nitrate

191 The annual deposition rate of atmospheric nitrate (D<sub>atm</sub>; total dry and wet deposition



192 rate of atmospheric nitrate) in each catchment was estimated using the annual “bulk”  
193 deposition rate of atmospheric nitrate ( $D_{\text{bulk}}$ ) calculated in Chiwa (2020) at each  
194 catchment by multiplying the volume-weighted mean concentration of nitrate in the  
195 bulk deposition samples collected every 2 weeks at each catchment for 10 years (from  
196 2009/1 to 2018/12) by the annual amount of precipitation. The bulk deposition samples  
197 were samples accumulated in a plastic bucket installed in an open site of each catchment  
198 55 cm above the ground. The concentrations of nitrate in these samples were measured  
199 by ion chromatography.

200 The  $D_{\text{bulk}}$  determined through this method, however, is less than  $D_{\text{atm}}$  (Aikawa et al.,  
201 2003) because the dry deposition velocities of gases and particles on the water surface  
202 of the plastic bucket are smaller than those on the forest (Matsuda, 2008). Thus, we  
203 corrected the differences by using Eq. (2) to estimate  $D_{\text{atm}}$  from  $D_{\text{bulk}}$ :

$$204 \quad D_{\text{atm}} = D_{\text{bulk}} - D_{\text{dry}}(\text{W}) + D_{\text{dry}}(\text{F}) \quad (2)$$

205 where  $D_{\text{dry}}(\text{W})$  and  $D_{\text{dry}}(\text{F})$  denote the annual dry deposition rates onto water and forest,  
206 respectively.

207 The  $D_{\text{dry}}(\text{W})$  and  $D_{\text{dry}}(\text{F})$  at each catchment were determined using an inferential  
208 method (Endo et al., 2011) through Eqs. (3) and (4), respectively:

$$209 \quad D_{\text{dry}}(\text{W}) = [\text{NO}_3^-]_{\text{atm, gas}} \times V_{\text{gas}}(\text{W}) + [\text{NO}_3^-]_{\text{atm, p}} \times V_{\text{p}}(\text{W}) \quad (3)$$

$$210 \quad D_{\text{dry}}(\text{F}) = [\text{NO}_3^-]_{\text{atm, gas}} \times V_{\text{gas}}(\text{F}) + [\text{NO}_3^-]_{\text{atm, p}} \times V_{\text{p}}(\text{F}) \quad (4)$$

211 where  $[\text{NO}_3^-]_{\text{atm, gas}}$  denotes the concentration of gaseous nitrate in air;  $[\text{NO}_3^-]_{\text{atm, p}}$   
212 denotes the concentration of particle nitrate in air;  $V_{\text{gas}}(\text{W})$  and  $V_{\text{gas}}(\text{F})$  denote the



213 deposition velocities of gaseous nitrate on the water surface and forest, respectively;  
214 and  $V_p(W)$  and  $V_p(F)$  denote the deposition velocities of particulate nitrate on the water  
215 surface and forest, respectively. Those determined by Chiwa (2010) using the annular  
216 denuder method from 2006/5 to 2007/4 were used for the  $[\text{NO}_3^-]_{\text{gas}}$  and  $[\text{NO}_3^-]_p$  in the  
217 FK catchments. Those determined by the National Institute for Environmental Studies  
218 (Environmental Laboratories Association of Japan, 2017) using the filter-pack method  
219 at Miyazaki (31°83'N, 131°42'E) from 2011 to 2017 were used for the  $[\text{NO}_3^-]_{\text{gas}}$  and  
220  $[\text{NO}_3^-]_p$  in the MY catchment. The  $V_{\text{gas}}(F)$ ,  $V_{\text{gas}}(W)$ ,  $V_p(F)$ , and  $V_p(W)$  of each  
221 catchment were determined by applying the estimation file for dry deposition (Matsuda,  
222 2008;

223 [http://www.hro.or.jp/list/environmental/research/ies/katsudo/acid\\_rain/kanseichinchaku](http://www.hro.or.jp/list/environmental/research/ies/katsudo/acid_rain/kanseichinchaku)  
224 [u/kanseichinchaku.html](http://www.hro.or.jp/list/environmental/research/ies/katsudo/acid_rain/kanseichinchaku)), where  $V_{\text{gas}}$  and  $V_p$  were calculated using the meteorological  
225 data of wind speed, temperature, humidity, radiation, and cloud amount and land use.  
226 The meteorological data monitored by Japan Meteorological Agency at the nearest  
227 Fukuoka station (33°34'N, 130°22'E) and Miyazaki station (31°56'N, 131°24'E) from  
228 2009 to 2018 were used for the FK and MY catchments, respectively. The forested land  
229 use of 100 % was chosen for each area.

230

## 231 2.5 Flux of stream water

232 The flux of stream water ( $F_{\text{stream}}$ ) in each catchment was not measured directly in this  
233 study. Instead, the water balance in each catchment was used to estimate  $F_{\text{stream}}$ ,



234 assuming that the outflux of water from the study catchments to deep groundwater was  
235 negligible:

$$236 \quad F_{\text{stream}} = P - E \quad (5)$$

237 where  $P$  denotes the annual average precipitation and  $E$  denotes the annual  
238 evapotranspiration flux of water in each catchment. In this paper, the equation obtained  
239 by Komatsu et al. (2008) was used to estimate the  $E$  of the FK and MY catchments.  
240 Details on this equation are shown below.

241 Komatsu et al. (2008) compiled the annual flux of evapotranspiration determined in  
242 43 forested catchments in Japan and found that  $E$  shows a positive correlation with the  
243 average temperature ( $T_{\text{avg}}$ ) of each catchment. Thus, they proposed the modeled relation  
244 of  $E \text{ (mm)} = 31.4T_{\text{avg}} \text{ (}^\circ\text{C)} + 376$  to estimate  $E$  in each forested catchment in Japan,  
245 where the standard error of 162.3 mm was included in the estimated evapotranspiration  
246 flux.

247

#### 248 2.6 Concentration of unprocessed $\text{NO}_3^-_{\text{atm}}$ in each water sample

249 The  $\Delta^{17}\text{O}$  data of nitrate in each sample was used to estimate the concentration of  
250  $\text{NO}_3^-_{\text{atm}}$  ( $[\text{NO}_3^-_{\text{atm}}]$ ) in each water sample by applying Eq. (6):

$$251 \quad [\text{NO}_3^-_{\text{atm}}]/[\text{NO}_3^-] = \Delta^{17}\text{O}/\Delta^{17}\text{O}_{\text{atm}} \quad (6)$$

252 where  $[\text{NO}_3^-_{\text{atm}}]$  and  $[\text{NO}_3^-]$  denote the concentrations of  $\text{NO}_3^-_{\text{atm}}$  and nitrate (total) in  
253 each water sample, respectively, and  $\Delta^{17}\text{O}_{\text{atm}}$  and  $\Delta^{17}\text{O}$  denote the  $\Delta^{17}\text{O}$  values of  
254  $\text{NO}_3^-_{\text{atm}}$  and nitrate (total) in the stream water sample, respectively. In this study, we



255 used the annual average  $\Delta^{17}\text{O}$  value of  $\text{NO}_3^-_{\text{atm}}$  determined at the Sado-Seki monitoring  
256 station in Japan (Sado Island; Fig. 1a) from April 2009 to March 2012 ( $\Delta^{17}\text{O}_{\text{atm}} =$   
257  $+26.3\text{‰}$ ; Tsunogai et al., 2016) for  $\Delta^{17}\text{O}_{\text{atm}}$  in Eq. (2) to estimate  $[\text{NO}_3^-_{\text{atm}}]$  in the stream.  
258 We allow for an error range of 3 ‰ in  $\Delta^{17}\text{O}_{\text{atm}}$ , where the factor changes in  $\Delta^{17}\text{O}_{\text{atm}}$   
259 from  $+26.3\text{‰}$  caused by both areal and seasonal variations in the  $\Delta^{17}\text{O}$  values of  
260  $\text{NO}_3^-_{\text{atm}}$  have been considered (Nakagawa et al., 2018; Tsunogai et al., 2016; Ding et  
261 al., 2022).

262 The annual export flux of unprocessed  $\text{NO}_3^-_{\text{atm}}$  per unit area of the catchment ( $M_{\text{atm}}$ )  
263 was determined by applying Eq. (7):

$$264 \quad M_{\text{atm}} = [\text{NO}_3^-_{\text{atm}}]_{\text{avg}} \times F_{\text{stream}} \quad (7)$$

265 where  $[\text{NO}_3^-_{\text{atm}}]_{\text{avg}}$  denotes the annual average  $[\text{NO}_3^-_{\text{atm}}]$  in each stream. The index of  
266 nitrogen saturation ( $M_{\text{atm}}/D_{\text{atm}}$  ratio) was calculated by dividing  $M_{\text{atm}}$  with  $D_{\text{atm}}$  in each  
267 catchment.

268

### 269 **3 Results**

#### 270 3.1 Deposition rate of atmospheric nitrate

271 Chiwa (2020) estimated the mean annual precipitation ( $P$ ) and mean annual  
272 temperature ( $T_{\text{avg}}$ ) to be 1769 mm and 15.9 °C, respectively, at FK catchments, and  
273 3837 mm and 10.8 °C, respectively, at MY catchment. Based on these data, the annual  
274 flux of stream water ( $F_{\text{stream}}$ ) was estimated to be  $893.7 \pm 162.3$  mm at FK catchments  
275 and  $3121.9 \pm 162.3$  mm at MY catchment, respectively, using Eq (5), corresponding to



276  $1.25 \times 10^5 \text{ m}^3/\text{year}$  in FK1,  $5.54 \times 10^5 \text{ m}^3/\text{year}$  in FK2, and  $1.34 \times 10^6 \text{ m}^3/\text{year}$  in MY.

277 Chiwa (2020) also reported the annual bulk deposition rates of atmospheric nitrate  
278 ( $D_{\text{bulk}}$ ) to be  $34.0 \text{ mmol m}^{-2} \text{ year}^{-1}$  at FK catchments and  $24.2 \text{ mmol m}^{-2} \text{ year}^{-1}$  at MY  
279 catchment. On the other hand, the annual dry deposition rate of atmospheric nitrate  
280 ( $D_{\text{dry}}$ ) deposited in the forest ( $D_{\text{dry}}(\text{F})$ ) and on the water surface ( $D_{\text{dry}}(\text{W})$ ) were  
281 estimated to be  $39.8 \text{ mmol m}^{-2} \text{ year}^{-1}$  and  $4.1 \text{ mmol m}^{-2} \text{ year}^{-1}$ , respectively, at FK  
282 catchments, and  $18.4 \text{ mmol m}^{-2} \text{ year}^{-1}$  and  $2.4 \text{ mmol m}^{-2} \text{ year}^{-1}$ , respectively, at MY  
283 catchment. As a result,  $D_{\text{atm}}$  was estimated to be  $69.3 \text{ mmol m}^{-2} \text{ year}^{-1}$  at FK catchments  
284 and  $40.1 \text{ mmol m}^{-2} \text{ year}^{-1}$  at MY catchments, using Eq. (2).

285

### 286 3.2 Concentration and isotopic composition of stream nitrate

287 The concentrations of stream nitrate at the FK1, FK2, and MY catchments ranged  
288 from  $97.5 \text{ }\mu\text{M}$  to  $121.3 \text{ }\mu\text{M}$ , from  $73.9 \text{ }\mu\text{M}$  to  $142.6 \text{ }\mu\text{M}$ , and from  $3.5 \text{ }\mu\text{M}$  to  $15.3 \text{ }\mu\text{M}$ ,  
289 respectively, with the average concentrations of  $109.5 \text{ }\mu\text{M}$ ,  $94.2 \text{ }\mu\text{M}$ , and  $7.3 \text{ }\mu\text{M}$ ,  
290 respectively (Fig. 2a). All catchments showed little seasonal variation during the  
291 observation periods. The variation ranges and the average concentrations of stream  
292 nitrate in the three catchments agreed well with the past observations performed in the  
293 same catchments (Chiwa, 2021).

294 The stable isotopic compositions of stream nitrate at the FK1, FK2, and MY  
295 catchments ranged from  $-0.9 \text{ ‰}$  to  $+1.5 \text{ ‰}$ , from  $-1.2 \text{ ‰}$  to  $+4.5 \text{ ‰}$ , and from  $-0.8 \text{ ‰}$   
296 to  $2.4 \text{ ‰}$ , respectively, for  $\delta^{15}\text{N}$  (Fig. 2b), from  $+3.9 \text{ ‰}$  to  $+8.5 \text{ ‰}$ , from  $-0.7 \text{ ‰}$  to



297 +3.6 ‰, and from -5.6 ‰ to +1.7 ‰, respectively, for  $\delta^{18}\text{O}$  (Fig. 2c), and from +2.0 ‰  
298 to +3.3 ‰, from +0.8 ‰ to +2.4 ‰, and from +0.2 ‰ to +1.0 ‰, respectively, for  $\Delta^{17}\text{O}$   
299 (Fig. 2d), with little seasonal variation during the observation periods. The  
300 concentration-weighted averages for the  $\delta^{15}\text{N}$ ,  $\delta^{18}\text{O}$ , and  $\Delta^{17}\text{O}$  values of stream nitrate  
301 were +0.2 ‰, +6.4 ‰, and +2.6 ‰, respectively, at FK1, +0.9 ‰, +1.7 ‰, and +1.7 ‰,  
302 respectively, at FK2, +0.7 ‰, -2.5 ‰, and +0.6 ‰, respectively, at MY. These values  
303 were typical for stream nitrate eluted from forested catchments (Hattori et al., 2019;  
304 Huang et al., 2020; Nakagawa et al., 2013, 2018; Riha et al., 2014; Sabo et al., 2016;  
305 Tsunogai et al., 2014, 2016).

306

307 3.3 Concentration of unprocessed atmospheric nitrate and the  $M_{\text{atm}}/D_{\text{atm}}$  ratio in each  
308 catchment

309 The concentration of unprocessed atmospheric nitrate ( $[\text{NO}_3^-]_{\text{atm}}$ ) in the streams of  
310 the FK1, FK2, and MY catchments ranged from 8.64 to 14.30  $\mu\text{M}$ , from 3.88 to 11.16  
311  $\mu\text{M}$ , and from 0.03 to 0.46  $\mu\text{M}$  with the average concentration of  $10.80 \pm 1.65$ ,  $6.09 \pm$   
312  $1.05$ , and  $0.16 \pm 0.05$   $\mu\text{M}$ , respectively, even though these study catchments showed  
313 little seasonal variations during the observation periods (Fig. 2e). The annual export  
314 flux of nitrate ( $M_{\text{total}}$ ), the annual export flux of  $\text{NO}_3^-$  ( $M_{\text{atm}}$ ), and the  $M_{\text{atm}}/D_{\text{atm}}$  ratio  
315 were  $97.9 \pm 17.8$   $\text{mmol m}^{-2} \text{ year}^{-1}$ ,  $9.7 \pm 2.3$   $\text{mmol m}^{-2} \text{ year}^{-1}$ , and  $13.9 \pm 4.3$  % at FK1  
316 catchment, respectively,  $84.2 \pm 15.3$   $\text{mmol m}^{-2} \text{ year}^{-1}$ ,  $5.4 \pm 1.4$   $\text{mmol m}^{-2} \text{ year}^{-1}$ , and  
317  $7.9 \pm 2.5$  % at FK2 catchment, respectively,  $22.6 \pm 1.2$   $\text{mmol m}^{-2} \text{ year}^{-1}$ ,  $0.5 \pm 0.1$   $\text{mmol}$





318  $\text{m}^{-2} \text{year}^{-1}$ , and  $1.2 \pm 0.4 \%$  at MY catchment, respectively (Table 2).

319

## 320 **4 Discussion**

### 321 4.1 Deposition rate of atmospheric nitrate at the study catchments

322 Based on the air monitoring data determined at the stations of Fukuoka ( $33^{\circ}51'N$ ,  
323  $130^{\circ}50'E$ ) and Miyazaki ( $31^{\circ}83'N$ ,  $131^{\circ}42'E$ ) from 2011 to 2017, the Environmental  
324 Laboratories Association of Japan (2017) reported  $D_{\text{atm}}$  to be  $57.8 \text{ mmol m}^{-2} \text{ year}^{-1}$  at  
325 Fukuoka and  $49.1 \text{ mmol m}^{-2} \text{ year}^{-1}$  at Miyazaki. Those values are consistent with the  
326  $D_{\text{atm}}$  estimated in this study ( $69.3$  and  $40.1 \text{ mmol m}^{-2} \text{ year}^{-1}$  at the FK and MY  
327 catchments, respectively), within a difference of approximately 20%. Thus, we  
328 concluded that the  $D_{\text{atm}}$  estimated in this study was reliable within the error margin of  
329 20% (Table 2). Because the  $D_{\text{atm}}$  determined at the FK catchments was the highest  
330 among the forested catchments in Table 3, we further compared the  $D_{\text{atm}}$  of the FK  
331 catchments with those from other air monitoring stations in Japan reported in past  
332 studies, along with that of the MY catchment (Table S1). While the  $D_{\text{atm}}$  of the MY  
333 catchment corresponded to the average level among the sites compiled in Table S1, the  
334  $D_{\text{atm}}$  of the FK catchments exceeded the average level significantly. In addition, the  $D_{\text{atm}}$   
335 of the FK catchments corresponded to one of the highest among the Japanese forested  
336 areas (Table S1). While all the catchments in this study can be suffered from the long-  
337 range transport of air pollutants derived from megacities in East Asian region (Chiwa,  
338 2021; Chiwa et al., 2012 and 2013), the shorter transport distance from the Fukuoka



339 metropolitan area (total population: 1.62 million people; population density: 4715  
340 people/km<sup>2</sup>) may be mainly responsible for the  $D_{\text{atm}}$  higher in FK than in MY, because  
341 the FK catchments are only 15 km west of the Fukuoka metropolitan area. As a result,  
342 the local emission in the Fukuoka metropolitan area should be responsible for the high  
343  $D_{\text{atm}}$  at the FK catchments.

344

#### 345 4.2 Excess leaching of unprocessed atmospheric nitrate from FK catchments

346 The striking features found in the FK catchments were that, in addition to the high  
347  $[\text{NO}_3^-]$  and high  $M_{\text{total}}$  clarified prior to this study (Chiwa, 2021), both  $[\text{NO}_3^-]_{\text{atm}}$  and  
348  $M_{\text{atm}}$  in FK were higher than those in MY (Table 2). Especially, the average  $[\text{NO}_3^-]_{\text{atm}}$   
349 in the FK1 stream was the highest ever reported in forested streams determined through  
350 continuous monitoring for more than 1 year (Bostic et al., 2021; Bourgeois et al., 2018b,  
351 2018a; Hattori et al., 2019; Huang et al., 2020; Nakagawa et al., 2018; Rose et al., 2015;  
352 Sabo et al., 2016; Tsunogai et al., 2014, 2016).

353 The observed high  $[\text{NO}_3^-]_{\text{atm}}$  in the FK1 stream could be caused by the high  $D_{\text{atm}}$ .  
354 Thus, we compiled all past data ever reported in forested streams through continuous  
355 monitoring in Table 3, where the data of average  $[\text{NO}_3^-]$ , average  $[\text{NO}_3^-]_{\text{atm}}$ ,  $M_{\text{atm}}$ ,  $M_{\text{total}}$ ,  
356  $D_{\text{atm}}$ , and  $M_{\text{atm}}/D_{\text{atm}}$  ratio were included for comparison, and the result showed that the  
357 FK1 catchment has the highest  $M_{\text{atm}}/D_{\text{atm}}$  ratio, along with  $M_{\text{atm}}$ , among the forested  
358 catchments (Table 3).

359 Elevated loading of nitrogen through atmospheric deposition was responsible for the



360 occurrence of nitrogen saturation in forest ecosystems, from which elevated levels of  
361 nitrate are exported (Aber et al., 1989). Nakagawa et al. (2018) proposed that the  
362  $M_{\text{atm}}/D_{\text{atm}}$  ratio can be an index for evaluating the nitrogen saturation in each forested  
363 catchment, because the  $M_{\text{atm}}/D_{\text{atm}}$  ratio directly reflects the present demand for  
364 atmospheric nitrate deposited in each forested catchment, and thus reflects the nitrogen  
365 saturation in each forested catchment. The high  $M_{\text{atm}}/D_{\text{atm}}$  ratios observed in the FK  
366 catchments implied that the stages of nitrogen saturation at the FK catchments were  
367 higher than those at other forested catchments, and thus, the nitrogen saturation at the  
368 FK catchments was responsible for the higher observed  $[\text{NO}_3^-]$  and  $M_{\text{total}}$  at the FK  
369 catchments than at MY and any other catchment ever studied (Table 3).

370 The stand age of forests can affect the retention or loss of N (Fukushima et al., 2011;  
371 Ohrui and Mitchell, 1997). Fukushima et al. (2011) evaluated N uptake rates of  
372 Japanese cedars at different ages (5-89 years old) and demonstrated that the N uptake  
373 rates of Japanese cedars were higher in younger stands ( $53 \text{ kg N ha}^{-1} \text{ year}^{-1}$  in 16 years  
374 old) than in older stands ( $29 \text{ kg N ha}^{-1} \text{ year}^{-1}$  in 31 years old;  $24 \text{ kg N ha}^{-1} \text{ year}^{-1}$  in 42  
375 years old;  $34 \text{ kg N ha}^{-1} \text{ year}^{-1}$  in 89 years old). In addition, Yang and Chiwa (2021)  
376 found that the nitrate concentration in the soil water taken beneath the rooting zone of  
377 matured artificial Japanese cedar plantations ( $607 \pm 59 \mu\text{M}$ ; 64-69 years old) was  
378 significantly higher than that of normal Japanese oak plantations ( $8.7 \pm 8.1 \mu\text{M}$ ; 24  
379 years old). Moreover, by adding ammonium nitrate ( $50 \text{ kg N ha}^{-1} \text{ year}^{-1}$ ) to the forest  
380 floor directly, Yang and Chiwa (2021) found that the nitrate concentration in the soil



381 water of the matured artificial Japanese cedar plantations increased significantly faster  
382 than that of the normal Japanese oak plantations, probably because of the lower N  
383 uptake rates in the matured artificial Japanese cedar plantations. Because most of the  
384 artificial Japanese cedar/cypress plantations in the FK and MY catchments have reached  
385 their maturity (> 50 years; Yang and Chiwa, 2021), the higher proportion of matured  
386 artificial Japanese cedar/cypress plantations in the FK1 catchment (Table 1) was highly  
387 responsible for the observed elevated leaching of nitrate caused by the reduction in N  
388 uptake rates.

389 As a result, we concluded that the FK forested catchments were under the high  
390 nitrogen saturation stage, FK1 catchment especially, and the high nitrogen saturation  
391 stage of the FK catchments was responsible for the elevated  $M_{\text{total}}$ ,  $M_{\text{atm}}$ ,  $[\text{NO}_3^-]$ ,  
392  $[\text{NO}_3^-_{\text{atm}}]$  found in the stream eluted from the catchment (Figs. 3a, 3b, and 3c).

393

#### 394 4.3 The $M_{\text{atm}}/D_{\text{atm}}$ ratio as an index of nitrogen saturation

395 Past studies have used the concentration of stream nitrate as one of the important  
396 indexes to evaluate the stage of nitrogen saturation in each forest (Aber, 1992; Huang  
397 et al., 2020; Rose et al., 2015; Stoddard, 1994). The strong linear relationship ( $R^2 = 0.81$ ;  
398  $P < 0.0001$ ) between the stream nitrate concentration and the  $M_{\text{atm}}/D_{\text{atm}}$  ratio, except  
399 for the Qingyuan forested catchment (Fig. 3d), further supported that the  $M_{\text{atm}}/D_{\text{atm}}$  ratio  
400 can be used as an alternative index of nitrogen saturation, as pointed out in Nakagawa  
401 et al. (2018). Moreover, the  $M_{\text{atm}}/D_{\text{atm}}$  ratio is a more reliable and robust index than the



402 stream nitrate concentration, as explained below.

403 The Qingyuan forested catchment can be classified into the highest nitrogen  
404 saturation stage based only on the highest stream nitrate concentration of 150  $\mu\text{M}$  (Table  
405 3). However, based on the leaching flux of nitrogen via stream water monitored by  
406 Huang et al. (2020) for 4 years in the Qingyuan forested catchment, along with the  
407 deposition flux of nitrogen, we can obtain the  $M_{\text{atm}}/D_{\text{atm}}$  ratio in the catchment to be a  
408 medium level of  $5.8 \pm 1.3 \%$ , implying that the nitrogen saturation stage was not very  
409 high (Table 3). Huang et al. (2020) also concluded that the input of nitrogen exceeded  
410 the output in the catchment, and thus, the catchment was at stage 2 of nitrogen saturation.  
411 The  $M_{\text{atm}}/D_{\text{atm}}$  ratio in the Qingyuan forested catchment with a medium level among all  
412 forested catchments (Fig. 3d) should be a more reliable index of nitrogen saturation.

413 Compared with those in the other forested catchments in Table 3, the annual amount  
414 of precipitation (P) has the lowest value of 709 mm in the Qingyuan forested catchment.  
415 The flux of stream water ( $F_{\text{stream}}$ ) has the lowest value of 309 mm as well. Thus, we  
416 concluded that nitrate was relatively concentrated in the catchment because of the small  
417 precipitation, resulting in relative enrichment in the concentrations of both nitrate (150  
418  $\mu\text{M}$ ) and unprocessed atmospheric nitrate (8.9  $\mu\text{M}$ ) in the stream.

419 While the concentration of stream nitrate, as an index of nitrogen saturation  
420 traditionally, can be influenced by the amount of precipitation, as demonstrated in the  
421 Qingyuan forested catchment, the  $M_{\text{atm}}/D_{\text{atm}}$  ratio is independent of the amount of  
422 precipitation (Fig. 4). Therefore, we concluded that the  $M_{\text{atm}}/D_{\text{atm}}$  ratio can be used as



423 a more robust index for evaluating nitrogen saturation in each forested catchment.

424

## 425 **5 Conclusions**

426 Both the concentrations and  $\Delta^{17}\text{O}$  of stream nitrate were determined for more than 2

427 years in the forested catchments of FK (FK1 and FK2) and MY to determine the

428  $M_{\text{atm}}/D_{\text{atm}}$  ratio for each catchment. The FK catchments exhibited higher  $M_{\text{atm}}/D_{\text{atm}}$  ratio

429 than the MY catchment and other forested catchments reported in past studies, implying

430 that the progress of nitrogen saturation in the FK catchments was severe. Both age and

431 proportion of artificial plantation in the FK catchments were responsible for the

432 progress of nitrogen saturation. In addition, although past studies have commonly used

433 the concentration of stream nitrate as an index to evaluate the progress of nitrogen

434 saturation in forested catchments, it can be influenced by the amount of precipitation.

435 As a result, we concluded that the  $M_{\text{atm}}/D_{\text{atm}}$  ratio should be used as a more reliable

436 index for evaluating the progress of nitrogen saturation because the  $M_{\text{atm}}/D_{\text{atm}}$  ratio is

437 independent from the amount of precipitation.

438

439 *Data availability.* All the primary data are presented in the Supplement. The other data

440 are available upon request to the corresponding author (Weitian Ding).

441

442 *Author contributions.* UT, FN, KS, and MC designed the study. MC and TK performed

443 the field observations. WD, UT, and FN determined the concentrations and isotopic



444 compositions of the samples. WD, TS, FN, and UT performed data analysis, and WD  
445 and UT wrote the paper with input from MC, TK, and KS.

446

447 *Competing interests.* The authors declare that they have no conflict of interest.

448

449 *Acknowledgements.*

450 We thank the Daisuke Nanki, Takuma Nakamura, and Yuko Muramatsu for their  
451 long-term water sampling. Additionally, we are grateful to the members of the  
452 Biogeochemistry Group, Graduate School of Environmental Studies, Nagoya  
453 University, for their valuable support throughout this study. This work was supported  
454 by a Grant-in-Aid for Scientific Research from the Ministry of Education, Culture,  
455 Sports, Science, and Technology of Japan under grant numbers 22H00561, and  
456 17H00780, the Yanmar Environmental Sustainability Support Association, and the  
457 River fund of the river foundation, Japan. Weitian Ding would like to take this  
458 opportunity to thank the ‘Nagoya University Interdisciplinary Frontier Fellowship’  
459 supported by JST and Nagoya University.

460

461

462

463

464



465 **Reference**

466 Aber, J. D.: Nitrogen cycling and nitrogen saturation in temperate forest ecosystems,

467 Trends Ecol. Evol., 7(7), 220–224, doi:10.1016/0169-5347(92)90048-G, 1992.

468 Aber, J. D., Nadelhoffer, K. J., Steudler, P. and Melillo, J. M.: Nitrogen Saturation in

469 Northern Forest Ecosystems, Bioscience, 39(6), 378–386, doi:10.2307/1311067,

470 1989.

471 Aikawa, M., Hiraki, T., Tamaki, M. and Shoga, M.: Difference between filtering-type

472 bulk and wet-only data sets based on site classification, Atmos. Environ., 37(19),

473 2597–2603, doi:10.1016/S1352-2310(03)00214-0, 2003.

474 Alexander, B., Hastings, M. G., Allman, D. J., Dachs, J., Thornton, J. A. and

475 Kunasek, S. A.: Quantifying atmospheric nitrate formation pathways based on a

476 global model of the oxygen isotopic composition ( $\delta^{17}\text{O}$ ) of atmospheric nitrate,

477 Atmos. Chem. Phys., 9(14), 5043–5056, doi:10.5194/acp-9-5043-2009, 2009.

478 Environmental Laboratories Association of Japan: Acid Rain National Survey Report

479 2017, [https://tenbou.nies.go.jp/envgis\\_explain/acid\\_rain/content.html](https://tenbou.nies.go.jp/envgis_explain/acid_rain/content.html).

480 Bostic, J. T., Nelson, D. M., Sabo, R. D. and Eshleman, K. N.: Terrestrial Nitrogen

481 Inputs Affect the Export of Unprocessed Atmospheric Nitrate to Surface Waters:

482 Insights from Triple Oxygen Isotopes of Nitrate, Ecosystems, doi:10.1007/s10021-

483 021-00722-9, 2021.

484 Bourgeois, I., Savarino, J., Némery, J., Caillon, N., Albertin, S., Delbart, F., Voisin,

485 D. and Clément, J. C.: Atmospheric nitrate export in streams along a montane to





486 urban gradient, *Sci. Total Environ.*, 633, 329–340,  
487 doi:10.1016/j.scitotenv.2018.03.141, 2018a.

488 Bourgeois, I., Savarino, J., Caillon, N., Angot, H., Barbero, A., Delbart, F., Voisin, D.  
489 and Clément, J. C.: Tracing the Fate of Atmospheric Nitrate in a Subalpine Watershed  
490 Using  $\Delta^{17}\text{O}$ , *Environ. Sci. Technol.*, 52(10), 5561–5570, doi:10.1021/acs.est.7b02395,  
491 2018b.

492 Chiwa, M.: Ten-year determination of atmospheric phosphorus deposition at three  
493 forested sites in Japan, *Atmos. Environ.*, 223(May 2019), 1–7,  
494 doi:10.1016/j.atmosenv.2019.117247, 2020.

495 Chiwa, M.: Long-term changes in atmospheric nitrogen deposition and stream water  
496 nitrate leaching from forested watersheds in western Japan, *Environ. Pollut.*,  
497 287(November 2020), 117634, doi:10.1016/j.envpol.2021.117634, 2021.

498 Chiwa, M., Enoki, T., Higashi, N., Kumagai, T. and Otsuki, K.: The Increased  
499 Contribution of Atmospheric Nitrogen Deposition to Nitrogen Cycling in a Rural  
500 Forested Area of Kyushu, Japan, *Water, Air, Soil Pollut.*, 224(11), 1763,  
501 doi:10.1007/s11270-013-1763-2, 2013.

502 Chiwa, M., Onikura, N., Ide, J. and Kume, A.: Impact of N-Saturated Upland Forests  
503 on Downstream N Pollution in the Tatara River Basin, Japan, *Ecosystems*, 15(2),  
504 230–241, doi:10.1007/s10021-011-9505-z, 2012.



505 Chiwa, M.: Characteristics of atmospheric nitrogen and sulfur containing compounds  
506 in an inland suburban-forested site in northern Kyushu, western Japan, *Atmos. Res.*,  
507 96(4), 531–543, doi:10.1016/j.atmosres.2010.01.001, 2010.

508 Ding, W., Tsunogai, U., Nakagawa, F., Sambuichi, T., Sase, H., Morohashi, M., and  
509 Yotsuyanagi, H.: Tracing the source of nitrate in a forested stream showing elevated  
510 concentrations during storm events, *Biogeosciences*, 19, 3247–3261,  
511 <https://doi.org/10.5194/bg-19-3247-2022>, 2022.

512 Endo, T., Yagoh, H., Sato, K., Matsuda, K., Hayashi, K., Noguchi, I. and Sawada, K.:  
513 Regional characteristics of dry deposition of sulfur and nitrogen compounds at  
514 EANET sites in Japan from 2003 to 2008, *Atmos. Environ.*, 45(6), 1259–1267,  
515 doi:10.1016/j.atmosenv.2010.12.003, 2011.

516 Fukushima, K., Tateno, R. and Tokuchi, N.: Soil nitrogen dynamics during stand  
517 development after clear-cutting of Japanese cedar (*Cryptomeria japonica*) plantations,  
518 *J. For. Res.*, 16(5), 394–404, doi:10.1007/s10310-011-0286-1, 2011.

519 Galloway, J. N., Aber, J. D., Erisman, J. W., Seitzinger, S. P., Howarth, R. W.,  
520 Cowling, E. B. and Cosby, B. J.: The nitrogen cascade, *Bioscience*, 53(4), 341–356,  
521 doi:10.1641/0006-3568(2003)053[0341:TNC]2.0.CO;2, 2003.

522 Hattori, S., Nuñez Palma, Y., Itoh, Y., Kawasaki, M., Fujihara, Y., Takase, K. and  
523 Yoshida, N.: Isotopic evidence for seasonality of microbial internal nitrogen cycles in  
524 a temperate forested catchment with heavy snowfall, *Sci. Total Environ.*, 690, 290–  
525 299, doi:10.1016/j.scitotenv.2019.06.507, 2019.



- 526 Hirota, A., Tsunogai, U., Komatsu, D. D. and Nakagawa, F.: Simultaneous  
527 determination of  $\delta^{15}\text{N}$  and  $\delta^{18}\text{O}$  of  $\text{N}_2\text{O}$  and  $\delta^{13}\text{C}$  of  $\text{CH}_4$  in nanomolar quantities from  
528 a single water sample, *Rapid Commun. Mass Spectrom.*, 24, 1085–1092,  
529 doi:10.1002/rcm.4483, 2010.
- 530 Huang, S., Wang, F., Elliott, E. M., Zhu, F., Zhu, W., Koba, K., Yu, Z., Hobbie, E.  
531 A., Michalski, G., Kang, R., Wang, A., Zhu, J., Fu, S. and Fang, Y.: Multiyear  
532 Measurements on  $\Delta^{17}\text{O}$  of Stream Nitrate Indicate High Nitrate Production in a  
533 Temperate Forest, *Environ. Sci. Technol.*, 54(7), 4231–4239,  
534 doi:10.1021/acs.est.9b07839, 2020.
- 535 Inoue, T., Nakagawa, F., Shibata, H. and Tsunogai, U.: Vertical Changes in the Flux  
536 of Atmospheric Nitrate From a Forest Canopy to the Surface Soil Based on  $\Delta^{17}\text{O}$   
537 Values, *J. Geophys. Res. Biogeosciences*, 126(4), 1–18, doi:10.1029/2020JG005876,  
538 2021.
- 539 Kaiser, J., Hastings, M. G., Houlton, B. Z., Röckmann, T. and Sigman, D. M.: Triple  
540 oxygen isotope analysis of nitrate using the denitrifier method and thermal  
541 decomposition of  $\text{N}_2\text{O}$ , *Anal. Chem.*, 79(2), 599–607, doi:10.1021/ac061022s, 2007.
- 542 Komatsu, D. D., Ishimura, T., Nakagawa, F. and Tsunogai, U.: Determination of the  
543  $^{15}\text{N}/^{14}\text{N}$ ,  $^{17}\text{O}/^{16}\text{O}$ , and  $^{18}\text{O}/^{16}\text{O}$  ratios of nitrous oxide by using continuous-flow  
544 isotope-ratio mass spectrometry Daisuke, *Rapid Commun. Mass Spectrom.*, 22, 1587–  
545 1596, doi:10.1002/rcm.3493, 2008a.
- 546 Komatsu, H., Maita, E. and Otsuki, K.: A model to estimate annual forest



547 evapotranspiration in Japan from mean annual temperature, , 330–340,  
548 doi:10.1016/j.jhydrol.2007.10.006, 2008b.

549 Konno, U., Tsunogai, U., Komatsu, D. D., Daita, S., Nakagawa, F., Tsuda, A.,  
550 Matsui, T., Eum, Y. J. and Suzuki, K.: Determination of total N<sub>2</sub> fixation rates in the  
551 ocean taking into account both the particulate and filtrate fractions, *Biogeosciences*,  
552 7(8), 2369–2377, doi:10.5194/bg-7-2369-2010, 2010.

553 Matsuda, K.: Estimation of dry deposition for sulfur and nitrogen compounds in the  
554 atmosphere : Updated parameterization of deposition velocity, *J. Japan Soc. Atmos.*  
555 *Environ.*, 43(6), 332–339, doi:10.11298/taiki1995.43.332, 2008.

556 McIlvin, M. R. and Altabet, M. A.: Chemical conversion of nitrate and nitrite to  
557 nitrous oxide for nitrogen and oxygen isotopic analysis in freshwater and seawater,  
558 *Anal. Chem.*, 77(17), 5589–5595, doi:10.1021/ac050528s, 2005.

559 Michalski, G., Scott, Z., Kabling, M. and Thiemens, M. H.: First measurements and  
560 modeling of  $\Delta^{17}\text{O}$  in atmospheric nitrate, *Geophys. Res. Lett.*, 30(16), 3–6,  
561 doi:10.1029/2003GL017015, 2003.

562 Michalski, G., Meixner, T., Fenn, M., Hernandez, L., Sirulnik, A., Allen, E. and  
563 Thiemens, M.: Tracing Atmospheric Nitrate Deposition in a Complex Semiarid  
564 Ecosystem Using  $\Delta^{17}\text{O}$ , *Environ. Sci. Technol.*, 38(7), 2175–2181,  
565 doi:10.1021/es034980+, 2004.

566 Mitchell, M. J., Iwatsubo, G., Ohru, K. and Nakagawa, Y.: Nitrogen saturation in  
567 Japanese forests: An evaluation, *For. Ecol. Manage.*, 97(1), 39–51,



568 doi:10.1016/S0378-1127(97)00047-9, 1997.

569 Morin, S., Sander, R. and Savarino, J.: Simulation of the diurnal variations of the  
570 oxygen isotope anomaly ( $\Delta^{17}\text{O}$ ) of reactive atmospheric species, *Atmos. Chem. Phys.*,  
571 11(8), 3653–3671, doi:10.5194/acp-11-3653-2011, 2011.

572 Nakagawa, F., Suzuki, A., Daita, S., Ohyama, T., Komatsu, D. D. and Tsunogai, U.:  
573 Tracing atmospheric nitrate in groundwater using triple oxygen isotopes: Evaluation  
574 based on bottled drinking water, *Biogeosciences*, 10(6), 3547–3558, doi:10.5194/bg-  
575 10-3547-2013, 2013.

576 Nakagawa, F., Tsunogai, U., Obata, Y., Ando, K., Yamashita, N., Saito, T.,  
577 Uchiyama, S., Morohashi, M. and Sase, H.: Export flux of unprocessed atmospheric  
578 nitrate from temperate forested catchments: A possible new index for nitrogen  
579 saturation, *Biogeosciences*, 15(22), 7025–7042, doi:10.5194/bg-15-7025-2018, 2018.

580 Nelson, D. M., Tsunogai, U., Ding, D., Ohyama, T., Komatsu, D. D., Nakagawa, F.,  
581 Noguchi, I. and Yamaguchi, T.: Triple oxygen isotopes indicate urbanization affects  
582 sources of nitrate in wet and dry atmospheric deposition, *Atmos. Chem. Phys.*, 18(9),  
583 6381–6392, doi:10.5194/acp-18-6381-2018, 2018.

584 Ohrui, K. and Mitchell, M. J.: Nitrogen Saturation in Japanese Forested Watersheds  
585 Author ( s ): Kiyokazu Ohrui and Myron J . Mitchell Published by : Wiley Stable  
586 URL : <http://www.jstor.org/stable/2269507> Accessed : 05-07-2016 04 : 51 UTC Your  
587 use of the JSTOR archive indicates your ac, , 7(2), 391–401, 1997.

588 Paerl, H. W. and Huisman, J.: Climate change: A catalyst for global expansion of



589 harmful cyanobacterial blooms, *Environ. Microbiol. Rep.*, 1(1), 27–37,  
590 doi:10.1111/j.1758-2229.2008.00004.x, 2009.

591 Peterjohn, W. T., Adams, M. B. and Gilliam, F. S.: Symptoms of nitrogen saturation  
592 in two central Appalachian hardwood forest ecosystems, *Biogeochemistry*, 35(3),  
593 507–522, doi:10.1007/BF02183038, 1996.

594 Riha, K. M., Michalski, G., Gallo, E. L., Lohse, K. A., Brooks, P. D. and Meixner, T.:  
595 High Atmospheric Nitrate Inputs and Nitrogen Turnover in Semi-arid Urban  
596 Catchments, *Ecosystems*, 17(8), 1309–1325, doi:10.1007/s10021-014-9797-x, 2014.

597 Rose, L. A., Elliott, E. M. and Adams, M. B.: Triple Nitrate Isotopes Indicate  
598 Differing Nitrate Source Contributions to Streams Across a Nitrogen Saturation  
599 Gradient, *Ecosystems*, 18(7), 1209–1223, doi:10.1007/s10021-015-9891-8, 2015.

600 Sabo, R. D., Nelson, D. M. and Eshleman, K. N.: Episodic, seasonal, and annual  
601 export of atmospheric and microbial nitrate from a temperate forest, *Geophys. Res.*  
602 *Lett.*, 43(2), 683–691, doi:10.1002/2015GL066758, 2016.

603 Stoddard, J. L.: Long-Term Changes in Watershed Retention of Nitrogen, , 223–284,  
604 doi:10.1021/ba-1994-0237.ch008, 1994.

605 Tsunogai, U., Komatsu, D. D., Daita, S., Kazemi, G. A., Nakagawa, F., Noguchi, I.  
606 and Zhang, J.: Tracing the fate of atmospheric nitrate deposited onto a forest  
607 ecosystem in Eastern Asia using  $\Delta^{17}\text{O}$ , *Atmos. Chem. Phys.*, 10(4), 1809–1820,  
608 doi:10.5194/acp-10-1809-2010, 2010.

609 Tsunogai, U., Daita, S., Komatsu, D. D., Nakagawa, F. and Tanaka, A.: Quantifying



610 nitrate dynamics in an oligotrophic lake using  $\Delta^{17}\text{O}$ , *Biogeosciences*, 8(3), 687–702,  
611 doi:10.5194/bg-8-687-2011, 2011.

612 Tsunogai, U., Komatsu, D. D., Ohyama, T., Suzuki, A., Nakagawa, F., Noguchi, I.,  
613 Takagi, K. and Nomura, M.: Quantifying the effects of clear-cutting and strip-cutting  
614 on nitrate dynamics in a forested watershed using triple oxygen isotopes as tracers, ,  
615 (1), 5411–5424, doi:10.5194/bg-11-5411-2014, 2014.

616 Tsunogai, U., Miyauchi, T., Ohyama, T., Komatsu, D. D., Nakagawa, F., Obata, Y.,  
617 Sato, K. and Ohizumi, T.: Accurate and precise quantification of atmospheric nitrate  
618 in streams draining land of various uses by using triple oxygen isotopes as tracers,  
619 *Biogeosciences*, 13(11), 3441–3459, doi:10.5194/bg-13-3441-2016, 2016.

620 Tsunogai, U., Miyauchi, T., Ohyama, T., Komatsu, D. D., Ito, M. and Nakagawa, F.:  
621 Quantifying nitrate dynamics in a mesotrophic lake using triple oxygen isotopes as  
622 tracers, *Limnol. Oceanogr.*, 63, S458–S476, doi:10.1002/lno.10775, 2018.

623 Vitousek, P. M. and Howarth, R. W.: Nitrogen limitation on land and in the sea: How  
624 can it occur?, *Biogeochemistry*, 13(2), 87–115, doi:10.1007/BF00002772, 1991.

625 Watanabe, M., Miura, S., Hasegawa, S., Koshikawa, M. K., Takamatsu, T., Kohzu,  
626 A., Imai, A. and Hayashi, S.: Coniferous coverage as well as catchment steepness  
627 influences local stream nitrate concentrations within a nitrogen-saturated forest in  
628 central Japan, *Sci. Total Environ.*, 636, 539–546, doi:10.1016/j.scitotenv.2018.04.307,  
629 2018.

630 Yamazaki, A., Watanabe, T. and Tsunogai, U.: Nitrogen isotopes of organic nitrogen



631 in reef coral skeletons as a proxy of tropical nutrient dynamics, *Geophys. Res. Lett.*,

632 38(19), 1–5, doi:10.1029/2011GL049053, 2011.

633 Yang, R. and Chiwa, M.: Low nitrogen retention in a Japanese cedar plantation in a

634 suburban area, western Japan, *Sci. Rep.*, 11(1), 1–7, doi:10.1038/s41598-021-84753-

635 1, 2021.

636

637

638

639

640

641

642

643

644

645

646

647

648

649

650

651





652 **Table 1.** Plant information for each forested catchment (Chiwa, 2021).

Overstory vegetation (%)	FK1	FK2	MY
Artificial Japanese cedar/cypress plantation	74	40	16
Other artificial coniferous plantations	<1	<1	7
Natural trees	10	54	75
Others	16	5	2

653

654

655 **Table 2.** Average concentrations of stream nitrate ( $[\text{NO}_3^-]_{\text{avg}}$ ), the average

656 concentrations of unprocessed  $\text{NO}_3^-_{\text{atm}}$  in streams ( $[\text{NO}_3^-_{\text{atm}}]_{\text{avg}}$ ), the annual export flux

657 of  $\text{NO}_3^-$  per unit area of catchments ( $M_{\text{total}}$ ), the annual export flux of  $\text{NO}_3^-_{\text{atm}}$  per unit

658 area of catchments ( $M_{\text{atm}}$ ), the deposition flux of  $\text{NO}_3^-_{\text{atm}}$  per unit area of catchment

659 ( $D_{\text{atm}}$ ), and the  $M_{\text{atm}}/D_{\text{atm}}$  ratios in the study catchments.

	FK1	FK2	MY
$[\text{NO}_3^-]_{\text{avg}}$ ( $\mu\text{M}$ )	109.5	94.2	7.3
$[\text{NO}_3^-_{\text{atm}}]_{\text{avg}}$ ( $\mu\text{M}$ )	$10.80 \pm 1.65$	$6.09 \pm 1.05$	$0.16 \pm 0.05$
$M_{\text{total}}$ ( $\text{mmol m}^{-2} \text{yr}^{-1}$ )	$97.9 \pm 17.8$	$84.2 \pm 15.3$	$22.6 \pm 1.2$
$M_{\text{atm}}$ ( $\text{mmol m}^{-2} \text{yr}^{-1}$ )	$9.7 \pm 2.3$	$5.4 \pm 1.4$	$0.5 \pm 0.1$
$D_{\text{atm}}$ ( $\text{mmol m}^{-2} \text{yr}^{-1}$ )	$69.3 \pm 13.9$	$69.3 \pm 13.9$	$40.1 \pm 8.0$
$M_{\text{atm}}/D_{\text{atm}}$ (%)	$13.9 \pm 4.3$	$7.9 \pm 2.5$	$1.2 \pm 0.4$

660

661

662

663

664

665



666 **Table 3.** The annual amount of precipitation (P), the average concentration of stream  
 667 nitrate ( $[\text{NO}_3^-]_{\text{avg}}$ ), the nitrogen saturation stage, the average concentration of  
 668 unprocessed  $\text{NO}_3^-_{\text{atm}}$  in streams ( $[\text{NO}_3^-_{\text{atm}}]_{\text{avg}}$ ), the annual export flux of  $\text{NO}_3^-$  per unit  
 669 area of catchment ( $M_{\text{total}}$ ), the annual export flux of  $\text{NO}_3^-_{\text{atm}}$  per unit area of catchment  
 670 ( $M_{\text{atm}}$ ), the deposition flux of  $\text{NO}_3^-_{\text{atm}}$  per unit area of catchment ( $D_{\text{atm}}$ ), and the  
 671  $M_{\text{atm}}/D_{\text{atm}}$  ratio in the FK1, FK2, and MY, along with those in the catchments studied in  
 672 past studies using  $\Delta^{17}\text{O}$  of nitrate as a tracer.

	P	$F_{\text{stream}}$	$[\text{NO}_3^-]_{\text{avg}}$	N stage*	$[\text{NO}_3^-_{\text{atm}}]_{\text{avg}}$	$M_{\text{atm}}$	$M_{\text{total}}$	$D_{\text{atm}}$	$M_{\text{atm}}/D_{\text{atm}}$
	mm	mm	$\mu\text{M}$		$\mu\text{M}$	$\text{mmol m}^{-2} \text{yr}^{-1}$			%
FK1 <sup>a</sup>	1769		109.5	-	10.8	9.7	97.9	69.3	13.9
FK2 <sup>a</sup>	1769		94.2	-	6.1	5.4	84.2	69.3	7.9
MY <sup>a</sup>	3837		7.3	-	0.2	0.5	22.6	40.1	1.2
KJ <sup>b</sup>	2500		58.4	-	3.3	4.3	76.4	45.6	9.4
IJ1 <sup>b</sup>	3300		24.4	2	1.4	2.9	50.1	44.5	6.5
IJ2 <sup>b</sup>	3300		17.1	-	0.6	1.2	35.1	44.5	2.6
Fernow1 <sup>c</sup>	1450		17.9	1	1.6	0.8	9.3	23.4	3.6
Fernow2 <sup>c</sup>	1450		34.3	2	3.4	1.5	14.8	23.4	6.3
Fernow3 <sup>c</sup>	1450		60.0	3	4.2	2.4	34.5	23.4	10.3
Uryu <sup>d</sup>	1170		0.7	-	0.1	0.1	1.0	18.6	0.7
Qingyuan <sup>e</sup>	709		150.0	2	8.9	2.9	49.3	50.0	5.8

673 a: This study

674 b: Nakagawa et al., 2018; Nakahara et al., 2010

675 c: Rose et al., 2015

676 d: Tsunogai et al., 2014

677 e: Huang et al., 2020

678 \*: N saturation stage estimated in past studies

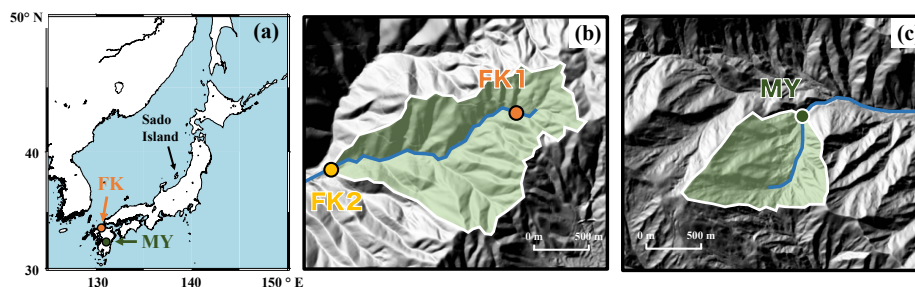
679 -: No data

680

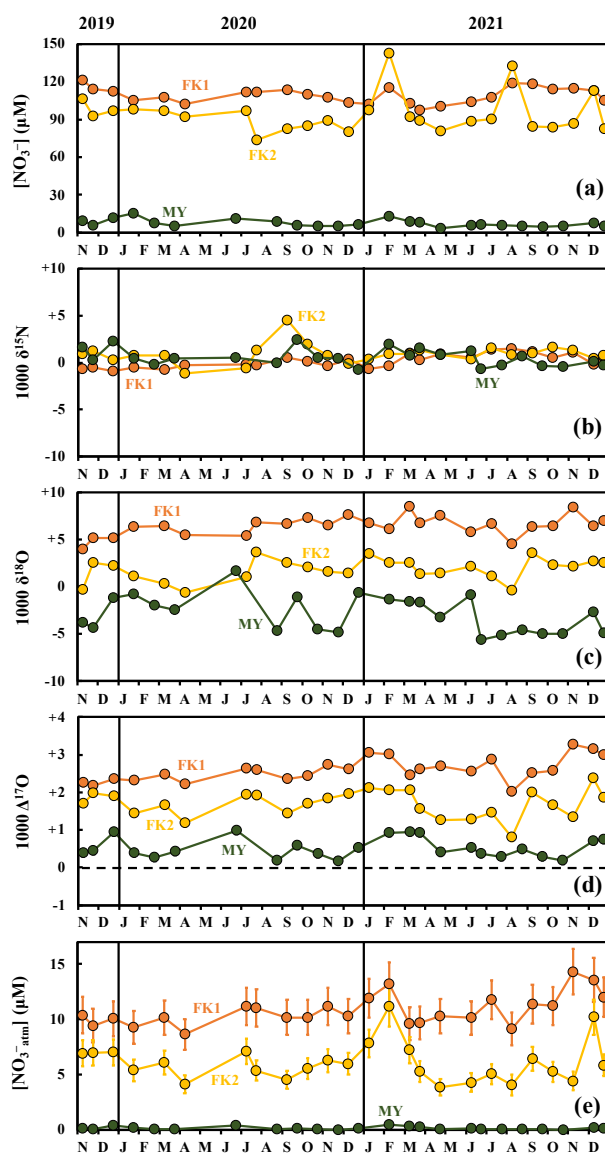
681

682

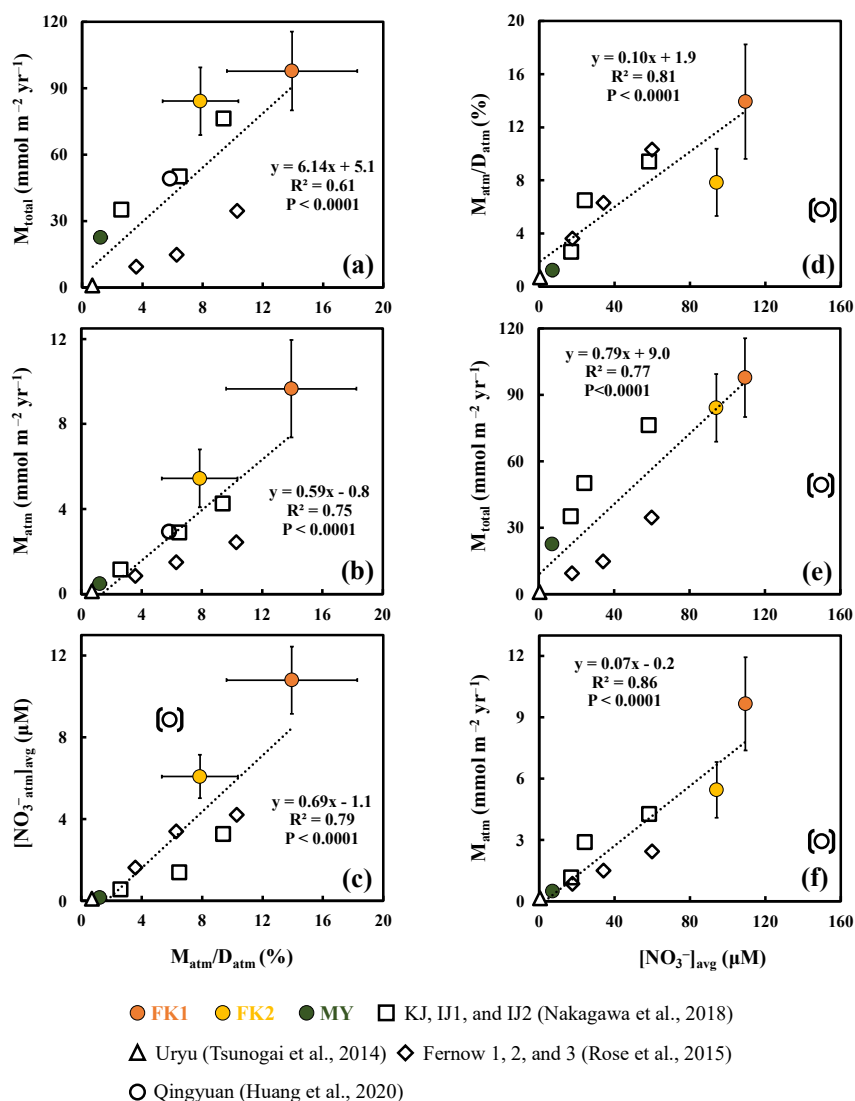
683



684 **Figure 1.** A map showing the locations of the study watersheds (FK and MY) in Japan  
685 (a), and the maps of FK1, FK2 (b) and MY catchments (c), together with the sampling  
686 point, shown by orange, yellow, and green circles, respectively.



687 **Figure 2.** Temporal variations in concentrations of stream nitrate (FK1: orange circles;  
 688 FK2: yellow circles; MY: green circles) (a), together with those in  $\delta^{15}N$  (b),  $\delta^{18}O$  (c),  
 689 and  $\Delta^{17}O$  (d) of nitrate, and the concentration of unprocessed  $NO_3^-_{atm}$  ( $[NO_3^-]_{atm}$ ) (e) in  
 690 the stream water of the FK1, FK2, and MY forested catchments. Error bars smaller than  
 691 the sizes of the symbols are not presented.



692

693 **Figure 3.** Annual export flux of nitrate per unit area ( $M_{total}$ ) plotted as a function of the

694  $M_{atm}/D_{atm}$  ratio in each forested catchment (a); the annual export flux of unprocessed

695 atmospheric nitrate per unit area ( $M_{atm}$ ) plotted as a function of the  $M_{atm}/D_{atm}$  ratio (b);

696 the average concentration of  $NO_3^-$  in the atmosphere ( $[NO_3^-]_{atm,avg}$ ) plotted as a function of the

697  $M_{atm}/D_{atm}$  ratio (c); the  $M_{atm}/D_{atm}$  ratio plotted as a function of the average concentration



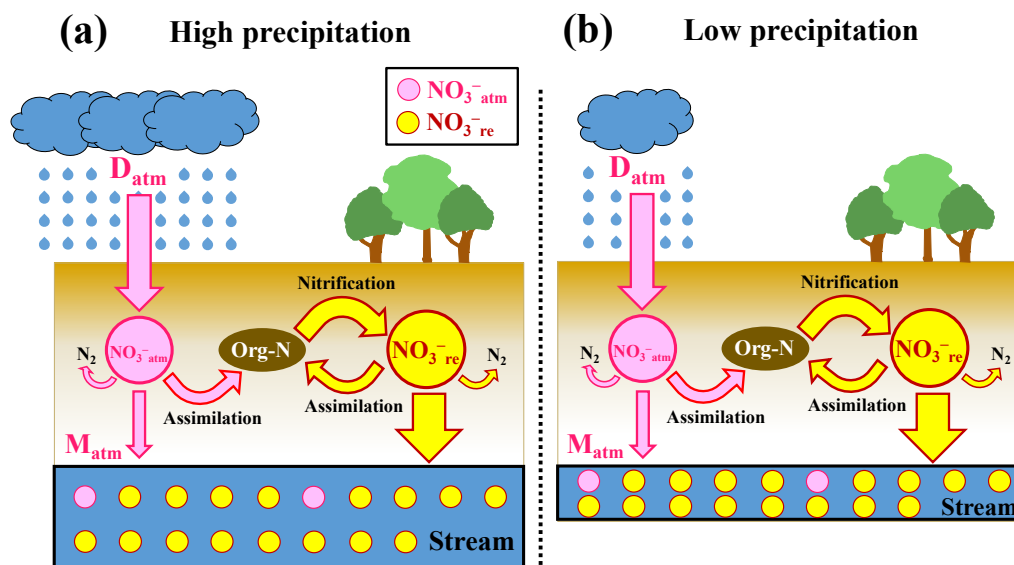
698 of nitrate ( $[\text{NO}_3^-]_{\text{avg}}$ ) (d); the  $M_{\text{total}}$  plotted as a function of  $[\text{NO}_3^-]_{\text{avg}}$  (e); the  $M_{\text{atm}}$   
699 plotted as a function of  $[\text{NO}_3^-]_{\text{avg}}$  (f) (FK1: orange circles; FK2: yellow circles; MY:  
700 green circles). Those determined for the forested catchments in past studies are plotted  
701 as well (Qingyuan: white circle (Huang et al., 2020); KJ, IJ1, and IJ2: white squares  
702 (Nakagawa et al., 2018); Fernow 1, 2, and 3: white diamonds (Lucy et al., 2015); Uryu:  
703 white triangle (Tsunogai., 2014)). The data obtained in the Qingyuan forested  
704 catchment are shown in parentheses and excluded from the calculation to estimate  
705 correlation coefficients (see text for the reason).

706

707

708

709



710 **Figure 4.** Schematic diagram showing the biogeochemical processing of nitrate in  
 711 forested catchments under high precipitation (a) and low precipitation (b), where  
 712  $\text{NO}_3^-_{\text{atm}}$  (unprocessed atmospheric nitrate) is represented by pink circles,  $\text{NO}_3^-_{\text{re}}$  by  
 713 yellow circles, the flows of  $\text{NO}_3^-_{\text{atm}}$  by pink arrows, and those of  $\text{NO}_3^-_{\text{re}}$  (remineralized  
 714 nitrate) by yellow arrows (modified after Nakagawa., 2018). Although the deposition  
 715 rates of  $\text{NO}_3^-_{\text{atm}}$  ( $D_{\text{atm}}$ ) and the biogeochemical reaction rates between (a) and (b) are  
 716 the same, we can expect high  $[\text{NO}_3^-]$  in (b). On the other hand, the  $M_{\text{atm}}/D_{\text{atm}}$  ratio  
 717 between (a) and (b) are the same.